An ultrahigh intensity laser at high repetition rate

J. Liu, H. Wang, J. Nees, D. Liu, O. Albert, B. Shan, G. Mourou, and Z. Chang
Center for Ultrafast Optical Science, University of Michigan, Ann Arbor, MI, 48109

We present an ultra intense laser system with high repetition rate (300 Hz) and good stability (1% RMS shot to shot fluctuation). By focusing the 21fs laser beam down to a 1.6 μm spot with aberration-compensated optics, we demonstrated that a peak intensity of 4×10^{18} W/cm^2 was produced with 2.5 mJ pulse energy. The intensity was confirmed by laser field ionization of argon atoms. With 8 fs pulses, focused intensity also exceeded 10^{18} W/cm^2 with 0.6 mJ pulse energy. By allowing the laser pulses to interact with solid targets, x-rays of up to 100 keV photon energy were produced with a 7 μm source size.

PACS numbers: 42.65.Re, 42.15.Fr, 42.60.Jf, 52.27.Ny, 52.38.–r, 52.70.La

1. INTRODUCTION

Following the invention of the chirped pulse amplification technique, the intensities of short pulse lasers have increased dramatically in the last fifteen years [1,2]. At the present, many lasers can reach the relativistic intensity level at which the quiver velocities of electrons in the laser field approach the speed of light. Such high intensity lasers provide powerful tools for developing sources of energetic electrons, ions, and x-rays with unique properties [3,4]. However, this regime could previously be reached only with relatively large and expensive lasers working at relatively low repetition rates, i.e., single-shot to 10 Hz [5,6]. The ultrahigh intensities of these lasers rely upon large pulse energies that are in the order of 100 mJ to several joules. We have showed that relativistic intensities can be produced with a few mJ ultrashort laser pulses. This was accomplished by focusing the laser beam to a wavelength scale spot with a small relative aperture mirror while its aberrations are corrected by adaptive optics. The high repetition rate operation of the laser and its superb stability provides opportunities to study high field science with high precision. We applied this new laser to the production of hard x-rays with small source size for high-resolution imaging.

2. THE LASER SYSTEM

A schematic diagram of the Ti:sapphire laser system is shown in Fig. 1. The front end is a prismless Ti:sapphire oscillator (FemtoLasers GmbH) that can generate sub-10-fs pulses. The pulses are then stretched to 40 ps by an all-reflective grating stretcher. A Faraday isolator is used to protect the oscillator from possible feedbacks from the amplifiers and experimental target. There are two Pockels cells in the system. The first one selects 300-Hz seed pulses and the second one enhances the contrast between the seed pulses and the unwanted prepulses that leak though the first Pockels cell. We measured the contrast with a fast photodiode and estimated the contrast to be in the order of 10^5.

The seed pulses are then injected into a multipass Ti:sapphire pre-amplifier. The pre-amplifier has seven passes and consists of only two curved mirrors. More than 1 mJ pulse energy can be obtained for a pump energy of 9.5 mJ from a frequency doubled diode-pumped Nd:YLF laser. The beam is then injected into the second amplifier, which has four passes.

Over 3.5 mJ pulse energy can be obtained for a pump energy of 17 mJ. After amplification, the laser pulses are compressed by a grating compressor. The output pulse energy is 2.5 mJ at 300 Hz. An autocorrelation measurement shows that the pulse has a FWHM of 21 fs, assuming a hyperbolic secant squared pulse shape.

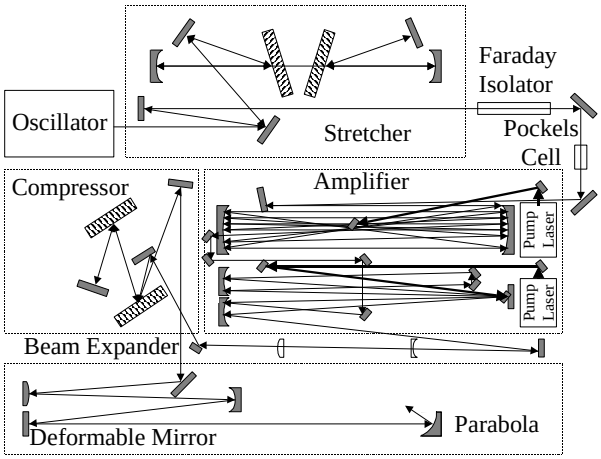

Fig. 1. Schematic diagram of the laser system.

In order to generate intensity greater than 10^{18} W/cm^2 with mJ pulses, an f/1 parabola is used to focus the laser beam. By definition, the focused intensity is $I \approx E/(\Delta t\ w^2)$, where E is the pulse energy, Δt is the pulse duration and w is the focal spot size. For a Gaussian beam, the beam radius is $w=(2/\pi)\, f\#\ \lambda$. Taking into account the clipping of laser beam due to the finite size of the optics, we estimated that the minimum spot size with f# = 1 is about 1 μm. However, we found that the parabola that we used has large aberrations. In fact, the surface shape of the mirror is so poor that it has two foci located 50 μm apart along the beam propagation direction. The beam shapes at these two foci are shown in Fig. 2. We believe that a portion of the mirror has a radius of curvature that is different from other part of the mirror. This mirror defect was probably associated with the way it was manufactured. The parabola we used was machined by the diamond-turned technique.

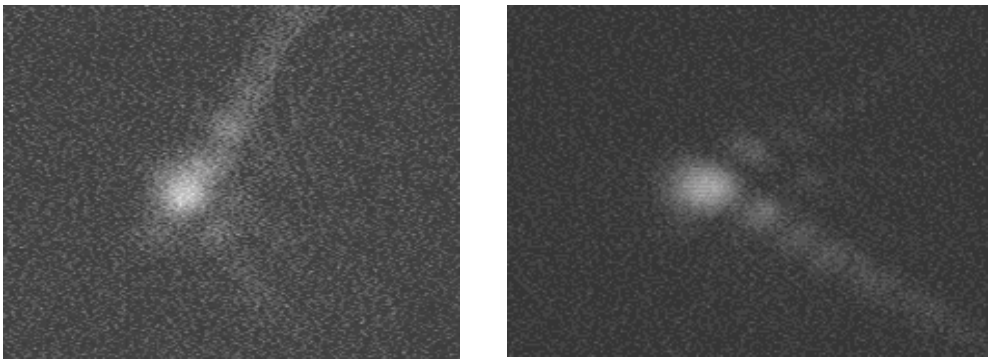

(a) The first focus (b) The second focus

Fig.2. Images of the laser beam at the two foci 50 μm apart along the propagation direction.

A deformable mirror was used to correct the aberrations of the f/1 parabola and the wavefront distortion from other parts of the laser system. The deformable mirror is a 2-inch-diameter silver mirror with 37 electrostrictive actuators (Xinetics). In conventional adaptive optical systems, one determines the optimal shape of the deformable mirror by first using a wavefront sensor to measure the wavefront distortion. He then calculates the needed mirror shape and feeds the information to the mirror controller to obtain a flat wavefront [7]. It is however extremely difficult to measure the wavefront of a beam focused by an f/1 parabola, so we developed a method that determines the optimal correction without the necessity of performing a wavefront measurement [8,9]. The scheme implemented here uses nonlinear optics in conjunction with machine learning through an evolutionary algorithm described below. Strong nonlinear effects occur at the focal spot of an ultrashort pulse. A stronger nonlinear signal generated at the focus corresponds to a smaller focal spot. Thus we can obtain diffraction-limited focusing by maximizing the nonlinear signal using the deformable mirror with no knowledge of the wavefront of the laser beam.

We implement the nonlinear correction scheme by using second-harmonic generation (SHG) in a thin β-barium borate crystal at the image of the focal spot. A 60X microscope objective is used to reduce the divergence of the beam to accommodate the acceptance angle of the SHG crystal. The SHG signal is used as the feedback for the computer-controlled deformable mirror. A genetic algorithm does the shape optimization of the deformable mirror. Good stability of the laser is crucial for the effectiveness of the nonlinear adaptive scheme, for otherwise the contributions of large laser energy fluctuations to the changes in the second harmonic generation signal would need to be eliminated somehow. The high repetition rate of the laser allows the genetic algorithm to converge a reasonable period of time (typically 20 to 30 minutes). In fact, we found that in our case the data acquisition and processing could not keep up with the laser repetition rate.

The magnified focal spot allows direct measurement of the spot size with a CCD camera. Figure 3 shows the close-to-diffraction-limited focal spot when the deformable mirror corrects the aberrations. The focal spot had a diameter of 1.6 μm at FWHM and 78% percent of the total energy is inside the $1/e^2$ radius, which leads to a peak intensity of 4×10^{18} W/cm^2.

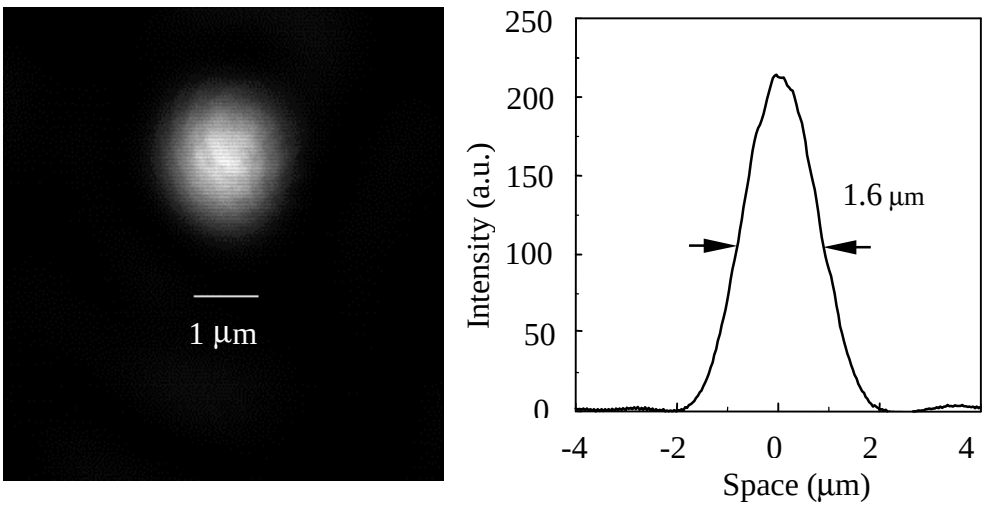

Fig. 3: Near diffraction limited focal spot with a diameter of 1.6 μm.

The laser intensity is also estimated by field ionization of noble gases with the focused beam. The intensity of our laser is so high that it can produce multiple charged state argon ions through tunneling ionization. In the tunneling regime, the ionization rate can be calculated quite accurately with the Ammosov-Delone-Krainov formula [10]. It gives that the threshold intensity of producing Ar^{9+} is above 10^{18} W/cm^2. The L shell ion spectra of argon obtained with our laser is shown in Fig. 4. It was measured with a time-of-flight ion spectrometer and a digital oscilloscope. Ionization stages up to Ar^{11+} were observed which indicate that the laser intensity is indeed in the middle 10^{18} W/cm^2 level.

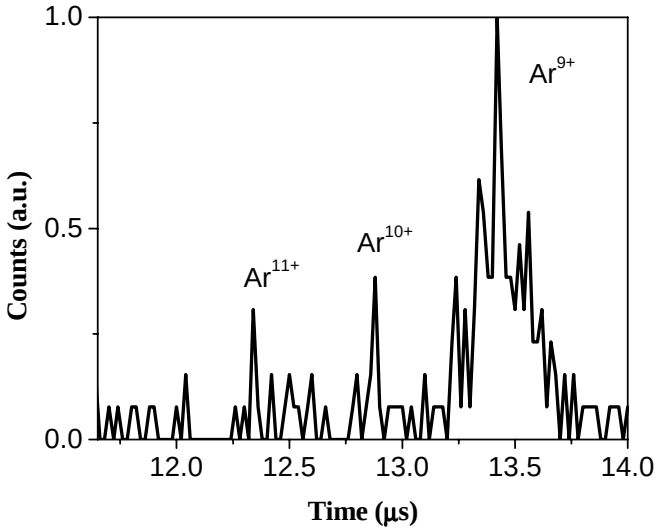

Fig. 4. The time-of-flight spectra of the L shell ion of argon

We also reached 10^{18} W/cm^2 intensity with sub-10 fs pulses [11]. The experiment was done with only the first stage amplifier. The 1.5 mJ pulses are compressed to 21 fs pulse duration and 1 mJ pulse energy by the grating compressor. The laser output is coupled into a hollow core fiber and chirped mirror pulses compressor system [12,13]. An 85cm long, 320 μm diameter hollow core fiber is kept straight in a V-groove on a cooper bar placed in a tube chamber that is filled with argon gas at 300 Torr pressure. The Kerr nonlinearity of argon imposes self-phase modulation (SPM) on the pulse propagating down the capillary. The input and output windows are fused silica flat substrates with a thickness of 0.5 mm oriented at the Brewster angle. This permits high transmission of broadband spectrum of input and output laser pulses. High order transverse modes were suppressed by the higher propagation loss that they experience in the leaky waveguide and by proper matching of the Gaussian input beam to the fundamental EH11 mode.

The output spectrum from the hollow core fiber extends from 700 to 900 nm. A pair of chirped mirrors is used to compensate the chirp induced by the SPM giving the 8 fs pulse duration with 0.6 mJ energy. A single-shot autocorrelation trace of the pulses is shown in Fig. 5. Pulse duration is calculated to be 8 fs by assuming a hyperbolic secant squared shape. A CCD camera measured the intensity profile of the beam exiting the fiber. The exiting beam profile is in single spatial mode. The beam is focused with the same parabola as used for the 21 fs laser and the aberrations are also corrected with the deformable mirror. The resulting spot is oval with a FHWM of 1.7x2 μm. 83% percent of the total energy is inside the $1/e^2$

radius. From the parameters of this system, a peak focal intensity of 1.7×10^{18}W/cm2 is generated.

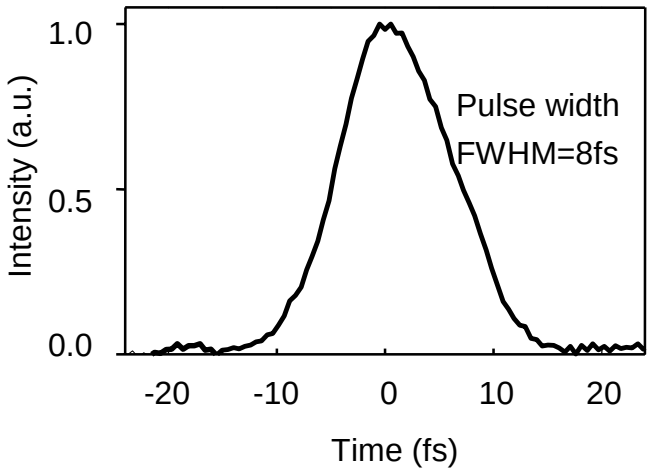

Fig. 5. An autocorrelation trace of the pulses obtained with the hollow-core fiber and chirped mirror compressor

3. HARD X-RAY GENERATION

In the last few years, ultrafast x-ray pulses from laser-solid interaction have emerged as powerful probes for time-resolved x-ray studies [14]. However, these x-ray sources are running at low repetition rates. Short pulse x-ray sources operating at high repetition rates will significantly speed up pump probe experiments. For high-resolution mammography, small animal imaging and some other medical applications, microfocused x-ray sources are desperately needed [15].

To generate characteristic line emissions around the 10 keV range, we chose Cu and Ge as the targets. The Cu targets are 4" diameter disks originally intended for use as vacuum gaskets. The Ge targets are 4" wafers designed for semiconductor applications. They are mounted on a motorized stage with two dimensions of translation and one rotation. The target stages are located inside a vacuum chamber pumped down to 10^{-6} Torr. The laser pulses used for the experiments are 21 fs long with about 1 mJ of energy. The x-ray spectrum was measured with a CZT photodiode connected to a multichannel analyzer. The solid angle in which the x-ray could reach the detector is controlled to minimize the possibility that two or more x-ray photons arrive on the detector during one laser shot. A typical x-ray spectrum from the Ge target is shown in Fig. 6, which consists of a strong $K\alpha$ line superimposed on a bremsstrahlung continuum. From this measurement we estimated that the x-ray flux is on the order of 10^7 photon/sec in a 2π solid angle.

The x-ray spot size was measured with both knife-edge imaging and slit imaging. Both measurements indicated the x-ray source is ~ 7 μm. The slit image is shown in Fig. 7, which is taken with an x-ray film using a 5 μm slit at 30X magnification. We consider the measured result as the upper bound of the real value for it is not trivial to measure an x-ray source of a few micrometers. To our knowledge, this is the smallest laser produced hard x-ray source size ever reported. The pulse duration of the x-ray is yet to be measured. We expect that it is on

the order of few hundred femtoseconds as has been measured in other laboratories under similar experimental conditions.

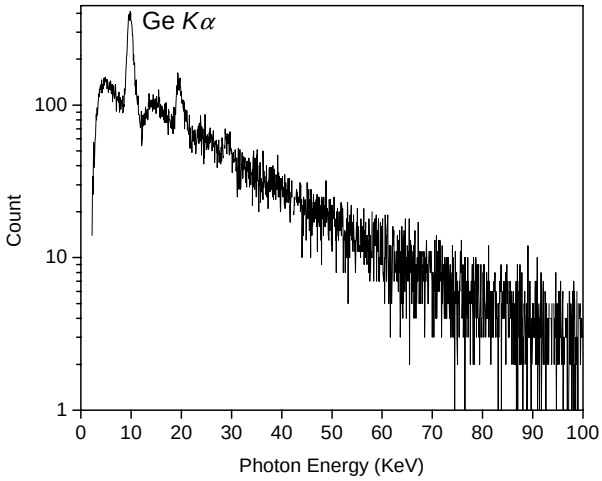

Fig.6. X-ray spectra from a Ge target

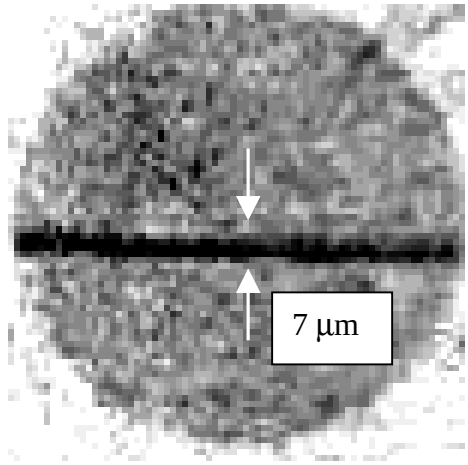

Fig.7. X-ray source imaged with a 5 μm slit

4. CONCLUSION

We have shown that by correcting the wavefront distortion with adaptive optics, a spot size of ~1 μm and intensities above 10^{18} W/cm^2 could be reached with femtosecond lasers operating at high repetition rates. Hard x-rays with 7 μm source size were produced by the interaction of the laser with solid targets.

ACKNOWLEDGEMENT

This work is supported by the National Science Foundation, the Department of Energy (grant No. DE-FG02-00ER15082) and the State of Michigan. The authors thank Peter Diehr for working on the English of the manuscript.

REFERENCES

[1] M. D. Perry and G. Mourou, Science **264,** 917 (1994).
[2] D. Strickland and G. Mourou, Opt. Commun. **56**, 219 (1985).
[3] M. D. Perry *et al.*, Rev. Sci. Instrum. **70**, 265 (1999).
[4] H. Schwoerer, P. Gibbon, S. Düsterer, R. Behrens, C. Ziener, C. Reich, and R. Sauerbrey, Phys. Rev. Lett. **86**, 2317 (2001).
[5] C. N. Danson, L. Barzanti, Z. Chang, A. Damerell, C.B. Edwards, S. Hankock, M.H.R.Hutchinson, M.H. Key, S. Luan, R. Mahadeo, I.P.Mercer, P.Norreys, D.A. Pepler, D.A. Rodkiss, I. Ross, M.A.Smith, R.A.Smith,P. Taday, W.T. Toner, K. Wigmore, R.W.W.Wyatt, F. Zhou, Opt. Commun. **103**, 392 (1993).
[6] M. D. Perry et. al., Opt. Lett. **24**, 160 (1999).
[7] F. Druon et. al., Opt. Lett. **23**, 1043 (1998).
[8] O. Albert, H. Wang, D. Liu, Z. Chang and G. Mourou, Opt. Lett. **25**. 1125 (2000).

[9] O. Albert et. al., Opt. Lett. **25**, 52 (2000).
[10] M. V. Ammosov, N. B. Delone and V. P. Krainov, Sov. Phys. JETP, **64,** 1191 (1986).
[11] D. Liu, J. Nees, H. Wang, G. Mourou, Z. Chang, and O. Albert, CLEO 2000 (Conference on Lasers and Electro-Optics), CPD5, San Francisco, May 7-12 (2000).
[12] M. Nisoli, S. De Silvestri and O. Svelto, Appl. Phys. Lett. **68**, 2793 (1996).
[13] M. Nisoli, S. De Silvestri, O. Svelto, R. Szipocs, K. Ferencz, Ch. Spielmann, S. Sartania and F. Krausz, Opt. Lett. **22**, 522 (1997).
[14] A. Rousse, C. Rischel, and J.C. Gauthier, Rev. Mod. Phys. **73**, 17(2001).
[15] R.W. Waynant, and I.K. Ilev, IEEE Journal on selected topics in quantum electronics, **6**, 1465 (2000).